Small-Angle Scattering of Neutrons by Heavy Nuclei*

F. T. KUCHNIR, A. J. ELWYN, J. E. MONAHAN, A. LANGSDORF, JR., AND F. P. MOORING
Argonne National Laboratory, Argonne, Illinois 60440
(Received 16 August 1968)

The differential cross sections and polarizations of neutrons elastically scattered by U, Th, Pb, Au, W, and Cd have been measured for scattering angles between 1.75° and 15°. The range of neutron energies covered is from 0.6 to 1.6 MeV. These data show no evidence for any anomalous long-range neutron-nucleus interaction. The data are used to evaluate an upper limit for the absolute value of the real part of the forward-scattering amplitude at each energy for each of the above scattering samples. The polarization of neutrons that emerge at 51° relative to the proton-beam direction in the ^{7}Li$(p,n)^7$Be reaction (the neutron-source reaction) is determined by use of these small-angle results for proton energies between 2.47 and 3.55 MeV. Some of the advantages of the use of small-angle neutron scattering as a polarization analyzer are discussed.

I. INTRODUCTION

ANY long-range contribution to the neutron-nucleus interaction is expected to manifest itself most clearly at small angles in the scattering of neutrons by nuclei. The known long-range forces are electromagnetic in origin. The only first-order electromagnetic interaction—that between the neutron's magnetic moment and the nuclear Coulomb field (Schwinger[1] interaction)—leads to an additional contribution to the differential scattering cross section and, through interference with the specifically nuclear amplitude, to large negative values of polarization in the small-angle region. On the other hand, the largest second-order contribution to the cross section and polarization at small angles is from the interaction[2] between the induced electric dipole moment of the neutron and the Coulomb field (polarizability interaction). This contribution is expected to be quite small[3,4] at a value of the neutron polarizability close to its experimentally determined[5] upper limit.

Some previous measurements[3,6] of the scattering of neutrons from heavy nuclei seemed to indicate that the differential cross section at small angles was larger than could be explained on the basis of a reasonable nuclear interaction plus the known electromagnetic contributions. Such apparently anomalous behavior has been reported, for example,[3] in the scattering of neutrons from U at 0.83 MeV and at various other energies between 2.0 and 14.0 MeV,[6,7] but not at 0.6 MeV.[4] It has been suggested[3,7] that this anomaly in U, if it exists, could be attributed to another long-range contribution to the neutron-nucleus interaction, and that it might be associated with the fission threshold.

The present experiment was undertaken in order to investigate the region of small angles in neutron scattering in more detail. To this end, the scattering from a number of heavy nuclei was studied at angles down to 1.75° and at a sequence of energies between 0.6 and 1.6 MeV. The experimental arrangement used in our earlier measurements[3] was modified somewhat to reduce possible systematic uncertainties in our previous study. Our hope was that a more accurate determination of cross sections and polarizations would lead to a better understanding of the effects arising both from the extranuclear and from the specifically nuclear contributions to the neutron-nucleus interaction at small scattering angles.

The organization of the present paper is as follows: Section II is a description of the experimental arrangement, the experimental procedure, and the results of the measurements. Section III is divided into three parts. In Sec. III A the measured cross sections and polarizations are compared with calculations[8] in which the neutron-nucleus interaction is represented by a potential containing terms corresponding to the magnetic-moment interaction (Schwinger scattering), the polarizability contribution, and the specifically nuclear interaction (optical-model potential). An optical-model potential is introduced to describe the (short-range) nuclear interaction for two reasons. First, the present angular and polarization distributions were measured only for scattering angles less than 15°, and the optical model provides a convenient representation in which these data can be related to other measurements at larger angles. Second, the values of the parameters that define an optical-model potential are of sufficient interest that it seemed worth while to investigate how sensitive

* Work performed under the auspices of the U. S. Atomic Energy Commission.

[1] J. Schwinger, Phys. Rev. **73**, 407 (1948).

[2] See, for example, V. S. Barashenkov and H. J. Kaiser, Fortschr. Physik **10**, 33 (1962), and references contained therein.

[3] A. J. Elwyn, J. E. Monahan, R. O. Lane, A. Langsdorf, Jr., and F. P. Mooring, Phys. Rev. **142**, 758 (1966).

[4] D. B. Fossan and M. Walt, Phys. Rev. Letters **12**, 672 (1964); M. Walt and D. B. Fossan, Phys. Rev. **137**, B269 (1965).

[5] Y. A. Aleksandrov, G. S. Samosvat, Zh. Sereter, and Tsoi Gen Sor, Zh. Eksperim. i Teor. Fiz. Pis'ma Redakstiya **4**, 196 (1966) [English transl.: JETP Letters **4**, 134 (1966)].

[6] Y. A. Aleksandrov, Zh. Eksperim. i Teor. Fiz. **33**, 294 (1957) [English transl.: Soviet Phys.—JETP **6**, 228 (1958)]; Y. A. Aleksandrov, G. V. Anikin, and A. S. Soldatov, Zh. Eksperim. i Teor. Fiz. **40**, 1878 (1961) [English transl.: Soviet Phys.—JETP **13**, 1319 (1961)]; Y. A. Aleksandrov and I. I. Bondarenko, Zh. Eksperim. i Teor. Fiz. **31**, 726 (1956) [English transl.: Soviet Phys.—JETP **4**, 612 (1957)].

[7] Y. V. Dukarevich and A. H. Dyumin, Zh. Eksperim. i Teor. Fiz. **44**, 130 (1963) [English transl.: Soviet Phys.—JETP **17**, 89 (1963)].

[8] J. E. Monahan and A. J. Elwyn, Phys. Rev. **136**, B1678 (1964).

the calculated values of the cross section and polarization for $\theta \lesssim 15°$ are to small changes of the optical-model potential. The absence of evidence for any anomalous long-range interaction is also noted in Sec. III A. Section III B describes the use of small-angle measurements to determine the forward (specifically nuclear) scattering amplitude and various limitations associated with such an analysis. Finally, in Sec. III C, the present left/right asymmetry results are used as a polarization analyzer to obtain modified values of the polarization $P_1(51°)$ of neutrons from the ^{7}Li$(p,n)^7$Be reaction.

II. EXPERIMENT

The differential cross sections and polarizations were systematically measured at a number of small angles by observing the scattering of a collimated beam of nearly monoenergetic neutrons. The energy range was 0.6–1.6 MeV and the scattering samples were U, Th, Pb, Au, W, and Cd. Since much of the experimental procedure is similar to that described in Ref. 3, the present description will be primarily concerned with the differences between the two experiments.

The experimental arrangement is shown schematically in Fig. 1 which indicates the relative positions of the neutron source, the scattering sample, and the neutron detectors and monitors. Partially polarized neutrons were produced in the ^{7}Li$(p,n)^7$Be reaction. A 20-μA proton beam from the Argonne 4.5-MeV Van de Graaff was incident on rotating evaporated-lithium-metal targets (about 50–80 keV thick) placed at the center of a shielded source tank. Partially polarized neutrons produced at 51° relative to the incoming proton beam passed between the poles of a spin-precession electromagnet and through a tapered rectangular collimator which was part of a previously designed source tank.[9] The beam size at the exit of the collimator (about 33 in. from the source spot) was $\frac{1}{2}\times\frac{1}{2}$ in. for a few runs ("small" collimator) and $\frac{1}{2}\times 1$ in. for most of the others ("large" collimator). The profile of the neutron beam emerging from the collimator was measured at the detector positions in both horizontal and vertical directions. For these measurements each detector was moved separately across the neutron beam, with its axis of symmetry perpendicular to the beam. The inset in Fig. 1 shows a horizontal-beam profile at a distance of about 70 in. from the exit of the collimator. The small tail observed on one of the sides is due to neutrons scattered into the scintillator from the photomultiplier when it intercepts the direct beam. In the present experiment, the smallest angle at which measurements were taken was 1.75°. For the "far" detectors (positioned approximately 70 in. from the collimator exit), this corresponds to a distance of ~4.5 cm from the center of the neutron beam to the center of the neutron detector. With no scatterer in place the ratio of the neutron flux measured at this position to that at the beam center was about 1 to 3000.

To compensate for low counting rates, measurements were taken at four scattering angles simultaneously. Each of the four detectors consisted of a cylindrical Stilbene scintillator 1 in. in length by 2 in. in diameter, directly coupled to an RCA-8575 photomultiplier specially aged and selected for low noise and afterpulsing.

The detector assemblies used in the "far" position could be moved parallel to their symmetry axes, along a track perpendicular to the neutron beam direction. These counters were used for measurements at angles $< 3°$. The "close" counters (positioned about 40 in. from the collimator exit) had their axes of symmetry perpendicular to a track which could rotate about a pivot at the scatterer position. The counter assemblies could slide along these radial tracks. The close counters were used for measurements at angles between 3° and 15°. The angular spread in the horizontal direction arose from the size of the detectors (~1° for the far counters and ~2° for the close ones) and from the 1.45° total spread of the collimated neutron beam.

A pulse-height spectrum of the recoil protons was taken at each incident neutron energy. The second group of neutrons from the ^{7}Li$(p,n)^7$Be* reaction to the first excited state at 430 keV in ^{7}Be could be identified and the detectors were biased to effectively eliminate it. γ-ray pulses with amplitudes greater than those for the most energetic recoil protons were also rejected by an upper-level discriminator. Pulse-shape discrimination was applied to reduce the high γ-ray background. The method (based on a zero-crossing technique) and the circuitry used, as well as the performance of the neutron-detection system, are described in detail by Kuchnir and Lynch.[10] At each bias setting, the energy dependence of the neutron detection efficiency was measured for each of the four detectors relative to the efficiency of a BF_3 long counter.

Each scattering sample was a cylinder positioned with its symmetry axis parallel to the neutron beam. The diameter was larger than the size of the collimated neutron beam and the thickness was chosen to give a transmission of approximately 0.60. Extreme care was taken during all of the runs to keep the proton beam from the Van de Graaff as steady as possible. The neutron flux emerging at a backward angle via a small opening in the shield tank was monitored by a BF_3 long counter. The forward neutron flux from the Li target was monitored by three $\frac{1}{2}\times\frac{1}{2}$-in. cylindrical Stilbene scintillators positioned about 165 in. from the collimator exit—one at the center of the neutron beam, the others midway along the beam profile at each side. The counting rate of each of the four monitors was recorded continuously.

[9] A. J. Elwyn, R. O. Lane, and A. Langsdorf, Jr., Phys. Rev. 128, 779 (1962), and references therein.

[10] F. T. Kuchnir and F. J. Lynch, IEEE Trans. Nucl. Sci. NS15, 107 (1968).

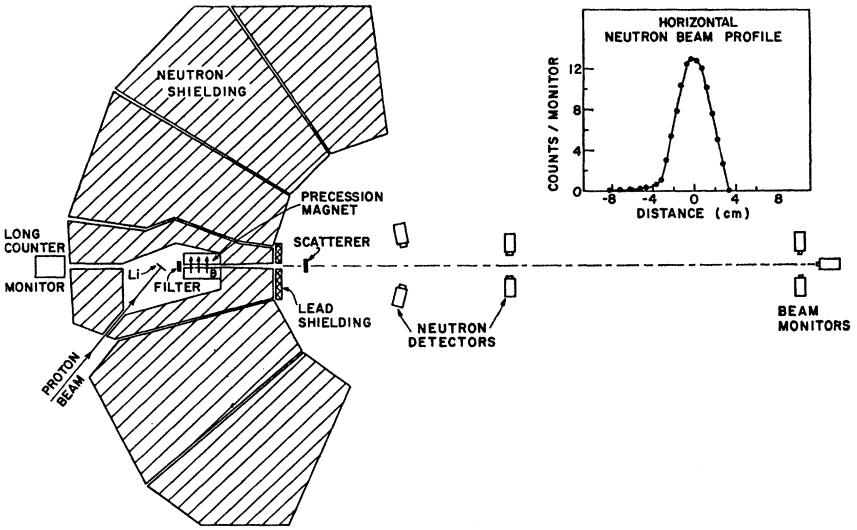

FIG. 1. Schematic diagram of the experimental arrangement. The use of filter sample is described in the text. The inset shows the horizontal neutron beam profile measured at a distance of about 70 in. from the collimator exit.

The main source of neutron background was the scattering by air particularly in the region near the detector. The background was therefore largest at the smallest scattering angles. In order to properly correct for this effect, and also for the possibility of an appreciable background contribution due to neutron scattering from the walls of the collimator, the background was measured with the scattering sample removed but with a "filter" sample of equal transmission placed between the neutron source and the entrance to the collimator. This is shown in Fig. 1. In this arrangement, the neutron-flux incident on the air column between the collimator exit and the detectors was very nearly the same as when the filter was removed and the scatterer put into place. Typical ratios of the counting rate with the scatterer in (filter out) to that with the scatterer out (filter in) were ~ 2 at 1.75°, ~ 3 at 4°, ~ 3.5 at 6°. These ratios were observed to be roughly independent of the neutron energy. Tests made with an evacuated pipe along the neutron-beam path indicated that 60% of the background at 1.75° was due to air scattering. This air-scattering background was halved when the detector was moved to an angle of 4°.

As mentioned earlier, data were collected at four angles simultaneously. At each angle we made four measurements—one for each of the four combinations of the scattering sample *in* or *out* and the spin-precession magnet *on* or *off*. An experimental point represents an average of at least one complete set of measurements (but usually many more) taken on each side of the neutron beam. This procedure was adopted in order to compensate for effects of possible asymmetries in the source-tank shielding, etc., on the two sides of the beam collimator.

Differential cross sections were obtained from the average of the measurements made with the precessing magnet on and off. These data were corrected for the effect of finite angular resolution (that is, for the effects of the spatial extension of the scatterer and detector), for multiple scattering of neutrons in the scattering samples, and for the presence of inelastically scattered neutrons. The incident neutron beam had a total angular spread of 1.45° in the horizontal direction and 1.45° (2.9°) in the vertical direction for the small (large) collimator. The finite angular resolution therefore necessitated quite an important correction to the differential cross section, especially at the very small angles where the cross sections associated with Schwinger scattering change rapidly over small angular regions. For the small collimator, this correction[11] increased the measured cross section by 12% at 1.75°, 5% at 2.5°, 3% at 4°, and 1% at 8°. For the large collimator, the correction reduced the measured cross section by $\sim 3\%$ for angles smaller than 4°, 2% at 4°, and 1% at 6°.

Corrections for multiple scattering in the scattering samples were estimated by use of a Monte Carlo program previously developed.[12] In each case, at least 5000 histories were traced and the distribution of neutrons arriving at the detector after one, two, or three collisions was recorded. From the Monte Carlo results, the ratio of the total number of scattered neutrons (corrected for the energy sensitivity of the detector) to the number of singly scattered neutrons was determined. This ratio was typically 1.1–1.2 for all of the elements studied. The contribution from inelastically scattered neutrons was evaluated from the known energy dependence of the detector efficiency

[11] The correction for finite angular resolution is briefly discussed in Ref. 3. The numerical evaluation of the four-dimensional integrals involved in these calculations is described by J. E. Monahan and A. J. Elwyn, Nucl. Instr. Methods **14**, 348 (1962); Argonne National Laboratory Report No. ANL-6420, 1961 (unpublished).

[12] R. O. Lane and W. F. Miller, Nucl. Instr. Methods **16**, 1 (1962).

TABLE I. Differential cross sections for elastic scattering of 0.6–1.6-MeV neutrons by U, Th, Pb, W, and Cd. The errors shown are based on counting statistics only.

Energy (MeV) \ Angle	1.75°	2.5°	4.0°	4.5°	6.0°	8.0°	10.0°	15.0°
Uranium								
0.6	2.78±0.12	2.30±0.06	1.80±0.05	2.04±0.06	1.95±0.04	1.71±0.04		1.94±0.07
0.84	2.98±0.07	2.50±0.09	2.26±0.05		2.19±0.04	2.12±0.04		1.99±0.07
1.0	2.73±0.08	2.74±0.10	2.18±0.08	2.12±0.04	2.26±0.06	1.95±0.05		
1.2	3.12±0.15	2.51±0.15		2.42±0.10	2.28±0.10	2.26±0.10		2.26±0.10
1.6	3.60±0.14	3.31±0.14		2.98±0.08	2.66±0.07	2.80±0.05		2.70±0.06
Thorium								
0.6	2.52±0.12	2.14±0.09		1.78±0.06	1.77±0.06	1.75±0.06		1.60±0.06
0.84	2.61±0.10	2.21±0.10		1.96±0.07	1.93±0.07	1.93±0.07		1.66±0.06
1.0	2.82±0.13	2.53±0.11		2.13±0.07	2.02±0.07	2.00±0.06		1.80±0.07
1.2	3.04±0.15	2.36±0.11		2.18±0.10	2.18±0.10	2.15±0.10		2.08±0.10
1.6	3.32±0.20	3.33±0.13		2.77±0.09	2.69±0.09	2.83±0.09	3.01±0.12	2.49±0.10
Lead								
0.84	2.17±0.08	2.03±0.06		1.81±0.06	1.78±0.05	1.79±0.05		1.58±0.05
Gold								
0.6	1.91±0.09	1.62±0.07		1.45±0.04	1.42±0.04	1.47±0.04		1.33±0.05
0.84	2.03±0.07	1.76±0.06		1.56±0.05	1.52±0.05	1.52±0.05		1.39±0.05
1.0	2.38±0.10	1.92±0.08		1.78±0.05	1.72±0.05	1.74±0.05		1.56±0.05
1.2	2.46±0.10	1.98±0.08		1.85±0.06	1.88±0.06	1.80±0.06		1.70±0.06
1.6	3.12±0.18	2.77±0.12		2.55±0.08	2.54±0.08	2.34±0.08	2.58±0.10	2.12±0.08
Tungsten								
0.84	2.45±0.09	2.12±0.07		1.98±0.07	1.88±0.06	1.91±0.06		1.71±0.06
1.0	2.94±0.13	2.40±0.11		2.18±0.07	2.19±0.07	2.10±0.07		2.02±0.08
1.2	2.73±0.14	2.38±0.11		2.25±0.09	2.13±0.08	2.17±0.08		1.94±0.08
Cadmium								
1.0	2.37±0.10	2.26±0.08		1.96±0.06	1.97±0.06	1.94±0.05		1.89±0.06

and the measured inelastic scattering cross sections[13] under the assumption that these neutrons are distributed isotropically in angle. Inelastic scattering contributed about 0.10 b/sr to the measured differential cross sections for U, Th, and W, about half as much for Au, and a negligible amount for Cd and Pb. The measured cross sections of U and Th were not corrected for the effect of fission neutrons since this contribution was estimated to be negligible for our experimental conditions.

Any further systematic effects, not specifically known, were taken into account by normalizing the data at each point to the known[14] cross section of polyethylene (CH_2). Measurements on polyethylene scatterers that had transmissions similar to the heavy samples of interest were taken at each energy under identical experimental conditions, and the cross sections were corrected for multiple scattering. The correction factors were typically 1.2–1.3. The final values of the differential elastic-scattering cross sections for 0.6–1.6-MeV neutrons incident on U, Th, Pb, Au, W, and Cd are given in Table I for angles between 1.75° and 15°. The errors shown are due to counting statistics only.

Polarization data were obtained from the ratio of neutrons detected first with zero field (magnet off) and then with the electromagnet turned on with its magnetic field adjusted to precess the neutron spins by 180°. This ratio is directly related to the product $P_1(51°)P(\theta)$, where $P_1(51°)$ is the polarization of the neutrons emitted at 51° in the $^7\mathrm{Li}(p,n)^7\mathrm{Be}$ reaction, and $P(\theta)$ is the polarization that results when unpolarized neutrons incident on the sample are elastically scattered at angle θ. The polarization $P(\theta)$ was obtained from the measured product by use of previously determined values[15] of $P_1(51°)$, and was corrected for the effect of finite angular resolution and inelastic scattering. When the large collimator was used, the correction for finite-size effects[11] increased the measured values of $P(\theta)$ by about 20% at 1.75°, about 10% for $2.5°<\theta<4.5°$, 5% at 6°, 3% at 8°, and 2% at 10°. With the small collimator, the effects of the correction were about half of the above. The presence of inelastically scattered neutrons introduced a correction of $\lesssim 5\%$ in the values of $P(\theta)$. The polarization data thus obtained (Table II) were not corrected for multiple scattering since no reliable estimate of this correction

[13] A. B. Smith, Nucl. Phys. **47**, 633 (1963); A. B. Smith, Phys. Rev. **126**, 718 (1962); A. M. de Villiers, C. A. Engelbrecht, W. G. Vonach, and A. B. Smith, Z. Physik **183**, 323 (1965); D. Lister, A. B. Smith, and C. Dunfold, Argonne National Laboratory Report No. ANL-7288, 1967 (unpublished); W. G. Vonach and A. B. Smith, Nucl. Phys. **78**, 389 (1966).

[14] D. J. Hughes and J. A. Harvey, Brookhaven National Laboratory Report No. BNL-325, 1955 (unpublished); Supplement (Superintendent of Documents, U. S. Government Printing Office, Washington, D. C., 1957).

[15] A. J. Elwyn and R. O. Lane, Nucl. Phys. **31**, 78 (1962). The values of $P_1(51°)$ used to obtain $P(\theta)$ shown in Table II are 0.255, 0.290, 0.320, 0.340, and 0.350 at 0.6, 0.84, 1.0, 1.2, and 1.6 MeV, respectively.

TABLE II. Values of the polarization for elastic scattering of 0.6–1.6-MeV neutrons from U, Th, Pb, Au, W, and Cd. The quantities listed here were obtained from the measured products $P_1(51°)P(\theta)$ by use of values for $P_1(51°)$ from Ref. 15. The errors shown are based on counting statistics alone.

Energy (MeV) \ Angle	1.75°	2.5°	4.0°	4.5°	6.0°	8.0°	10.0°	15.0°
Uranium								
0.6	−0.40±0.11	−0.34±0.06	−0.42±0.08	−0.29±0.07	−0.18±0.03	−0.20±0.04		−0.10±0.06
0.84	−0.49±0.06	−0.43±0.08	−0.26±0.05		−0.24±0.04	−0.14±0.03		−0.11±0.05
1.0	−0.61±0.05	−0.40±0.08	−0.31±0.06	−0.29±0.02	−0.23±0.03	−0.18±0.03		
1.2	−0.55±0.08	−0.65±0.08		−0.37±0.06	−0.26±0.06	−0.18±0.06		−0.03±0.06
1.6	−0.71±0.08	−0.62±0.06		−0.37±0.05	−0.15±0.04	−0.19±0.03		−0.11±0.03
Thorium								
0.6	−0.52±0.13	−0.35±0.11		−0.36±0.08	−0.31±0.08	−0.12±0.07		−0.10±0.07
0.84	−0.58±0.11	−0.24±0.07		−0.27±0.06	−0.24±0.06	−0.10±0.06		−0.10±0.05
1.0	−0.37±0.15	−0.60±0.13		−0.39±0.07	−0.19±0.07	−0.04±0.07		−0.03±0.06
1.2	−0.64±0.11	−0.51±0.10		−0.40±0.06	−0.21±0.06	−0.24±0.06		−0.12±0.05
1.6	−1.03±0.13	−0.63±0.10		−0.46±0.07	−0.38±0.07	−0.15±0.06	−0.09±0.07	−0.03±0.06
Lead								
0.84	−0.42±0.09	−0.31±0.08		−0.29±0.06	−0.16±0.06	−0.11±0.06		−0.18±0.05
Gold								
0.06	−0.61±0.13	−0.22±0.12		−0.40±0.08	−0.30±0.07	+0.01±0.08		−0.04±0.06
0.84	−0.44±0.10	−0.50±0.08		−0.12±0.06	−0.16±0.06	−0.22±0.06		−0.07±0.05
1.0	−0.43±0.11	−0.45±0.11		−0.14±0.07	−0.26±0.07	−0.21±0.07		−0.05±0.06
1.2	−0.78±0.09	−0.45±0.08		−0.41±0.06	−0.20±0.06	−0.19±0.06		−0.10±0.05
1.6	−0.72±0.13	−0.56±0.11		−0.46±0.07	−0.15±0.07	−0.21±0.07	−0.15±0.07	−0.13±0.06
Tungsten								
0.84	−0.36±0.10	−0.22±0.08		−0.16±0.05	−0.18±0.05	−0.13±0.04		−0.14±0.04
1.0	−0.65±0.14	−0.43±0.13		−0.19±0.07	−0.16±0.07	−0.14±0.07		−0.07±0.06
1.2	−0.55±0.11	−0.54±0.10		−0.18±0.05	−0.17±0.05	−0.13±0.05		−0.02±0.05
Cadmium								
1.0	−0.24±0.18	−0.40±0.10		−0.15±0.06	−0.18±0.04	−0.08±0.04		−0.04±0.04

is available. However, the correct values of $P(\theta)$ should lie well within the experimental errors indicated in the table.

III. DISCUSSION

A. Calculations

The measured cross sections and polarizations shown in Tables I and II have been compared with calculations with a potential based on a formalism developed in Refs. 3 and 8. The advantage of such a formalism over the usual Born-approximation methods is that all terms in the potential are taken into account correctly through first order in the long-range (perturbation) potential. In these calculations the neutron-nucleus interaction includes the long-range electromagnetic terms —both magnetic-moment contributions (Schwinger scattering) and the contributions due to an induced electric dipole moment (polarizability)—as well as a term due to the specifically nuclear force, approximated for these medium and heavy nuclei by an optical-model potential.

Since the nuclear scattering largely determines the magnitude of the differential cross section at angles down to about 3°–4°, it is useful to investigate the sensitivity with which both the calculated cross sections and polarization respond to variation of the parameters of the optical model. We have calculated these quantities for a number of proposed optical-model potentials that have been used with more or less success to describe the large-angle cross section and polarization measurements for nuclei throughout the periodic table. The potentials investigated were those of Rosen,[16] Perey and Buck,[17] Bjorklund and Fernbach,[18] and Auerbach and Moore.[19] In these models, the real well is represented by

$$V(r)=-Vf(r)-iWg(r)+V_s\left(\frac{\hbar}{m_\pi c}\right)^2\left[\frac{1}{r}\frac{d}{dr}f(r)\right]\boldsymbol{\sigma}\cdot\mathbf{l}, \quad (1)$$

with $f(r)=\{1+\exp[(r-R)/a_s]\}^{-1}$. The imaginary potential was of the surface-absorption type with the form factor $g(r)$ given either as a Gaussian[18,19]

$$g(r)=\exp[-(r-R)/a_d]^2,$$

or as a surface derivative[16,17]

$$g(r)=4\left(1+\exp\frac{r-R}{a_d}\right)^{-2}\exp\frac{r-R}{a_d}.$$

[16] L. Rosen, in *Proceedings of the International Conference, Antwerp, 19–23 July 1965*, edited by M. Né ve de Mévergnies, P. VanAssche, and J. Vervier (North-Holland Publishing Co., Amsterdam, 1966), p. 380.

[17] F. Perey and B. Buck, Nucl. Phys. **32**, 353 (1962).

[18] F. J. Bjorklund and S. Fernbach, Phys. Rev. **109**, 1295 (1958).

[19] E. H. Auerbach and S. O. Moore, Phys. Rev. **135**, B895 (1964).

The parameters for the models of Refs. 16–18 are summarized by Rosen.[16] The parameters of the optical model of Auerbach and Moore are the values given in Ref. 19.

The results of these calculations for U at 1.2 MeV are given in Fig. 2, in which the large-angle values are based on calculations with the code ABACUS-2,[20] and the small-angle quantities are from computations based on the formalism of Monahan and Elwyn[3,8] with the polarizability $\alpha \approx 10^{-41}$ cm. In this comparison of the predicted cross sections and polarizations at small angles, note that the values based on the various models differ from each other only in magnitude. The major discrepancies among the four models arise at angles greater than $\sim 20°$.

The optical model of Auerbach and Moore[19] provides good average fits to a variety of scattering data at large angles for heavy nuclei. With this as a reference potential, we have calculated the small-angle cross sections and polarizations to study their sensitivity to individual changes in the model parameters. Figure 3 illustrates the effects of varying the real-well depth V, the imaginary depth W, and the spin-orbit depth V_s, one at a time. At angles less than 20° both the polarization and cross sections are quite insensitive to rather large changes in V, W, and V_s, and the observed differences are primarily differences in magnitude only. Other calculations of the polarization with $V_s = 0$ yield results indistinguishable from the values shown in Fig. 3(c) for $\theta \lesssim 10°$. Variations in the geometric parameters a_s and R associated with the real well (Fig. 4) produce somewhat larger changes in the calculated cross sections and polarizations, although the specific parameter variations shown here are perhaps unreasonably large. In these computations, both the spin-orbit radius and diffuseness parameter are set equal to those for the real well. Other calculations in which the spin-orbit radius is made smaller than R produce virtually no change in the results for $\theta \lesssim 25°$.

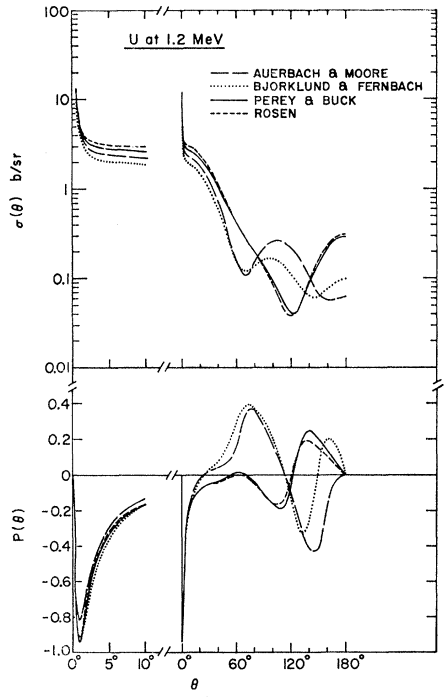

FIG. 2. Calculated differential cross section and polarization for neutrons scattered by U at 1.2 MeV for the various optical potentials indicated.

[20] E. H. Auerbach, Brookhaven National Laboratory Report No. BNL-6562, 1962 (unpublished).

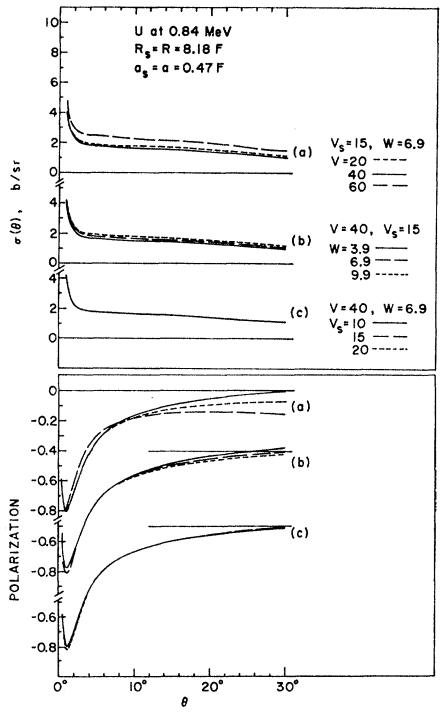

FIG. 3. Calculated differential cross sections and polarizations for neutrons scattered by U at 0.84 MeV for individual changes in some of the parameters of the optical model of Ref. 19. The parameter being changed is the real-well depth V for curves (a), the imaginary depth W for curves (b), and the spin-orbit well depth V_s for curves (c).

In general, then, both the cross sections and (especially) the polarizations are rather insensitive to changes in the optical-model parameters at angles less than 20° (at least when they are varied one at a time), except perhaps to variation of the radius of the real well. Even for reasonable changes in this parameter, the fractional changes in the polarization are somewhat smaller than the corresponding changes in the cross sections. It should be emphasized that for all nuclei the polarization at angles less than about 10° is independent of the nuclear spin-orbit potential. This arises from the fact that the amplitude associated with the magnetic-moment interaction completely dominates the nuclear spin-orbit amplitude at these small angles.

The optical model of Auerbach and Moore was used to represent the nuclear interaction in calculations based on the formalism of Ref. 8. In these computations the polarizatility of the neutron was taken to be $\alpha = 10^{-41}$ cm^3,[21] a value only slightly greater than the upper limit of 6×10^{-42} cm^3 given by Aleksandrov *et al.*[5] In Fig. 5 the measured cross sections from Table I (points) are compared with the calculations (smooth curves) as a function of angle and energy for each of the nuclei. The factors near unity on the smooth curves are scale factors by which the calculations had to be multiplied to obtain reasonable agreement with the data. The effect of such a normalization is equivalent to a small change in one or more of the optical-model parameters since such changes have only a small effect on the shapes of the curves.

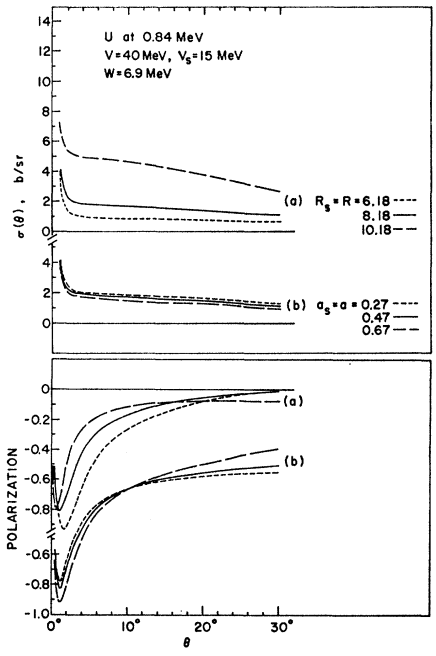

FIG. 4. Calculated differential cross sections and polarizations for neutrons scattered by U at 0.84 MeV for individual changes in some of the parameters of the optical model of Ref. 19. The curves marked (a) refer to changes in the real-well radius R. Those marked (b) refer to changes in the real-well diffuseness a. The corresponding spin-orbit well parameters R_s and a_s are set equal to the real-well values.

The over-all good agreement between the measurements and the calculations—which, as mentioned, are based on the "known" contributions to the neutron-nucleus interaction—offers little support for the anomalous behavior reported in earlier experiments. This absence of anomalous behavior is even more evident in Fig. 6, in which the measured cross sections minus the contribution from Schwinger scattering are compared with calculations based on a scattering potential that includes only the terms due to nuclear and polarizability interactions. The angular dependence exhibited by the data is in good agreement with the shapes of the calculated curves. Thus, the general systematic trend for all nuclei provides evidence that there is no anomaly in the measured small-angle cross sections at energies below 1.6 MeV. In a careful experiment on a number of

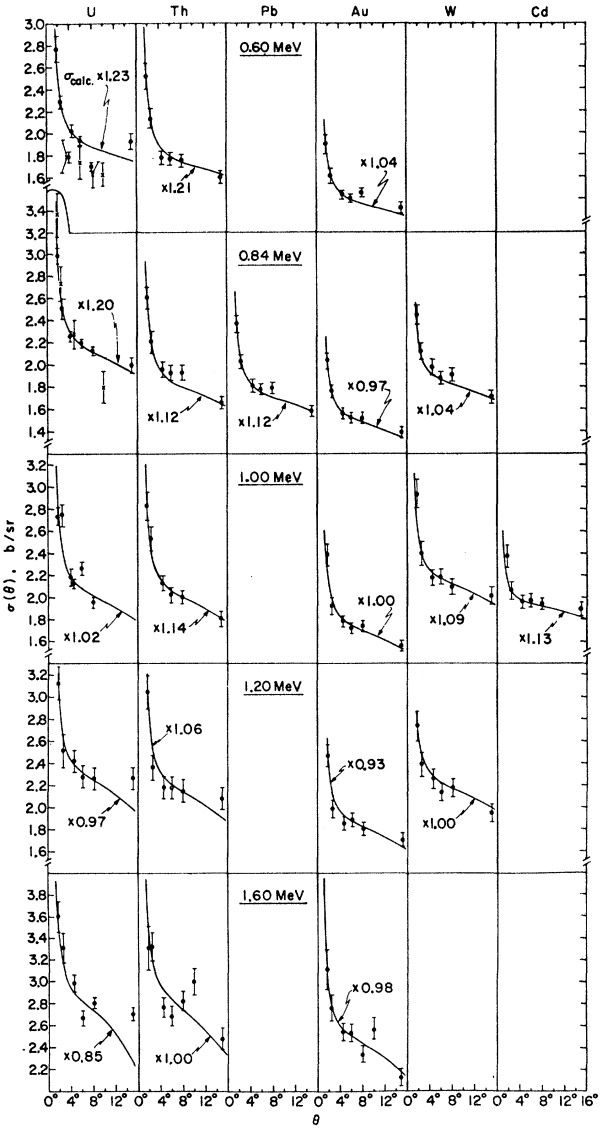

FIG. 5. Differential cross sections for neutrons scattered by U, Th, Pb, Au, W, and Cd at energies between 0.6 and 1.6 MeV. The experimental values (points) are from Table I. The smooth curves are calculations based on the formalism described in Refs. 3 and 8 for $\alpha = 10^{-41}$ cm^3. The factors near unity shown on the smooth curves are scale factors by which the calculations had to be multiplied to obtain agreement with the measurements. The data points plotted as x's for U are from Ref. 3 (0.84 MeV) and Ref. 4 (0.6 MeV).

[21] The use of measured small-angle cross sections to determine the polarizability α has been discussed previously (Ref. 3). It was pointed out that, because of ambiguities in the optical-model potential, such measurements cannot lead to an accurate limit on the polarizability for values of $\alpha \leqslant 10^{-41}$ cm^3.

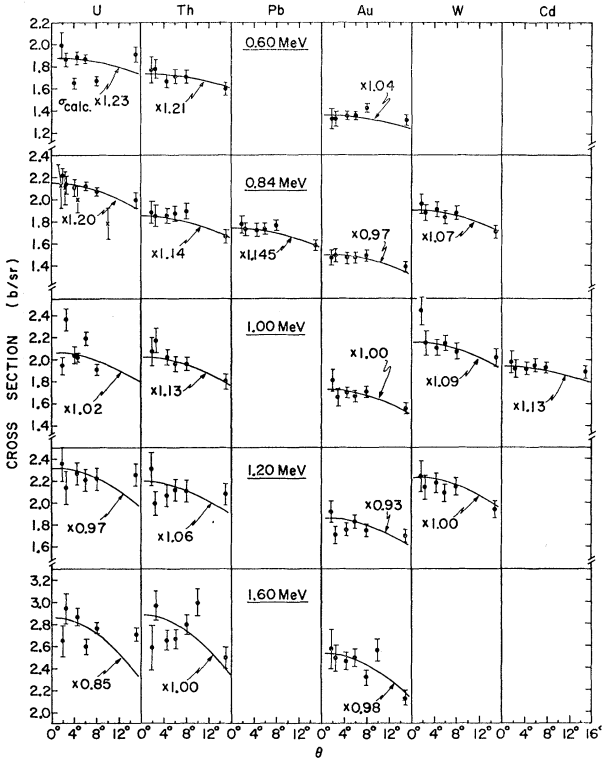

FIG. 6. Differential cross sections for neutrons scattered by U, Th, Pb, Au, W, and Cd at energies between 0.6 and 1.6 MeV minus the contribution from Schwinger scattering. The smooth curves are calculations based on the formalism of Refs. 3 and 8 with a potential that includes only the nuclear and polarizability interactions for $\alpha=10^{-41}$ cm^3. The factors near unity are described in the caption for Fig. 5 and in the text. The data points × for U at 0.84 MeV are from Ref. 3.

nuclei, Gorlov *et al.*[22] also find no evidence for anomalous behavior in measured small-angle cross sections at an energy of 4 MeV.

As seen in Figs. 5 and 6, the present results for U at 0.84 MeV are in reasonable agreement with the previous measurements[3] at 0.83 MeV except perhaps near 10°. The tentative interpretation of the earlier results as evidence for an anomaly in the cross section was based on the differences between the measured and the calculated values of the slope of the differential cross section, the calculated values being normalized to the measurement at $\theta=15°$ (Fig. 9 of Ref. 3). On the basis of the present experiment, however, no such systematic difference is observed. The present results (Fig. 6) indicate that the measured cross sections minus Schwinger contributions are almost independent of angle for $\theta\lesssim10°$. It might be noted that if the dashed curve in Fig. 9 of Ref. 3 were scaled upward instead of being normalized to the experimental cross section at 15°, its interpretation as an indication of anomalous behavior would be much less likely.

[22] G. V. Gorlov, N. S. Lebedeva, and V. M. Morozov, Zh. Eksperim. i Teor. Fiz. Pis'ma Redakstiya **5**, 131 (1967) [English transl.: JETP Letters **5**, 106 (1967)].

The measured values of the polarization are compared with calculations in Fig. 7. Although the observed and calculated angular dependences agree, the observed magnitude of the polarization at energies less than 1 MeV is systematically smaller than the calculated values and at 1.6 MeV the measured values are systematically larger. These effects are similar for all of the scattering samples, and since the calculated values of the polarization are quite insensitive to variations in the parameters of the nuclear potential, the observed trends suggest the need for modification of the values used for the neutron polarization $P_1(51°)$ in the source reaction. In any event, the over-all agreement in the angular dependence of the measured and calculated values of polarization is consistent with the absence of anomalous behavior in the data. This is in agreement with the previous measurement at 0.83 MeV. Since this conclusion is based on the angular dependence of the polarization product $P_1(51°)P(\theta)$, it is independent of the actual value used for $P_1(51°)$.

Rather detailed attempts to fit the magnitudes of the measured small-angle cross sections without scale factors, were made by use of the parameter-space scan routines in the ABACUS-2 computer program. Better absolute fits to the differential cross sections for U from 0.6 to 1.6 MeV were obtained for real-well depths which, at energies greater than 1.0 MeV, are 2% larger than the Auerbach-Moore parameters and at the lower energies are 10–12% smaller. For all energies a real-well radius 2.5% larger than the original value was required. While these changes improved the fits to the measured cross sections, the calculated values of the polarizations were affected only slightly. These modifications in the parameters of the model potential should not, however, be considered too significant, since any complete parameter-space scan must utilize large-angle data as well as the measurements at small angles. Thus, while the scale factors shown in Figs. 5 and 6 can be accounted for through these changes, the energy dependence of the real-well parameters does not seem realistic. Furthermore, it might be emphasized that these modifications do not account for the systematic discrepancies between measured and calculated values of the polarization.

B. Nuclear Scattering Amplitudes

Here we consider the extent to which the real and imaginary parts of the forward-scattering amplitude can be evaluated from small-angle measurements of the kind described above.

The amplitude for the scattering of a neutron at an angle θ by a spin-zero nucleus can be written as

$$f(\theta)=g(\theta)+h(\theta)\boldsymbol{\sigma}\cdot\mathbf{n}, \qquad (2)$$

where $\mathbf{n}$ is the unit vector normal to the scattering plane and $\boldsymbol{\sigma}$ is the Pauli spin vector. It is convenient to express each of the amplitudes $g(\theta)$ and $h(\theta)$ as a sum

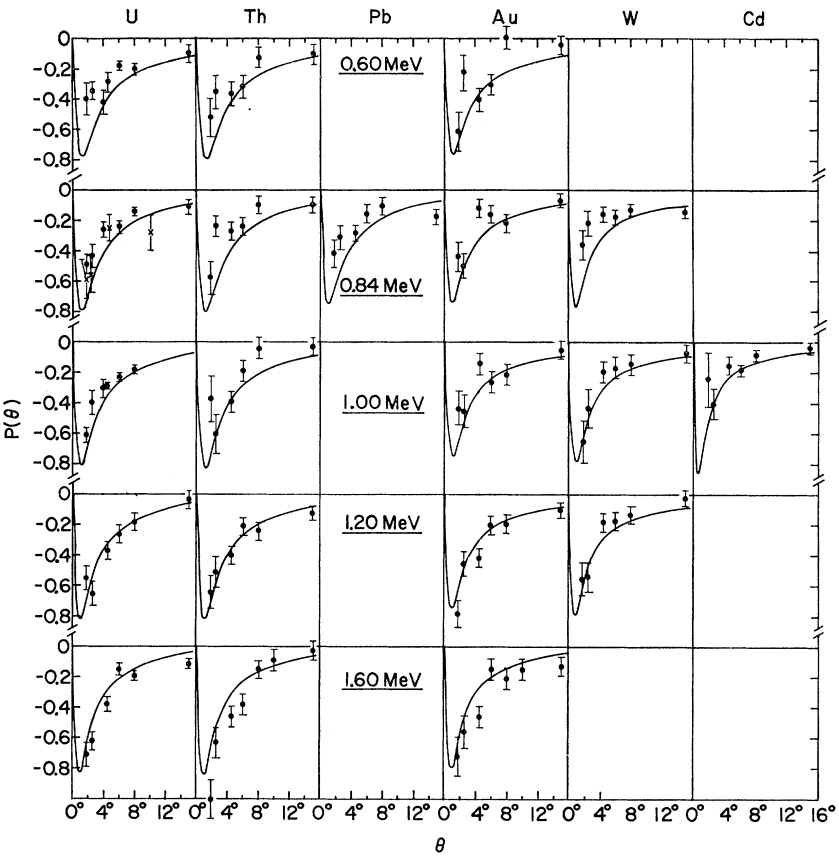

FIG. 7. The polarization for neutrons scattered by U, Th, Pb, Au, W, and Cd at energies between 0.6 and 1.6 MeV. The experimental results (points) are from Table II. The smooth curves are calculations based on the formalism of Refs. 3 and 8 for $\alpha=10^{-41}$ cm^3. The data points $\times$ for U at 0.84 MeV are from Ref. 3.

of the contributions $g_n(\theta)$ and $h_n(\theta)$ from the specifically nuclear interaction and the contributions $g_s(\theta)$ and $h_s(\theta)$ from the electromagnetic interaction. For values of $\alpha\lesssim 10^{-41}$ cm^3, the polarizability interaction can be neglected so that the electromagnetic interaction is assumed to be entirely given by the Schwinger term. As emphasized in Sec. III A, for values of θ close to zero, the contribution to $f(\theta)$ from spin-dependent nuclear forces becomes negligibly small so that $h_n(\theta)$ can be set equal to zero. Further, the calculated values of $g_s(\theta)$ and $\mathrm{Re}h_s(\theta)$ become vanishingly small as θ approaches zero. Thus, for $\theta\lesssim\theta_0$, where θ_0 is some small angle, it follows that $h_n(\theta)\approx g_s(\theta)\approx \mathrm{Re}h_s(\theta)\approx 0$, and Eq. (2) becomes

$$f(\theta)=g_n(\theta)+i\,\mathrm{Im}h_s(\theta)\boldsymbol{\sigma}\cdot\mathbf{n}, \quad \theta\lesssim\theta_0. \tag{3}$$

The corresponding cross section and polarization are

$$\sigma(\theta)=|g_n(\theta)|^2+[\mathrm{Im}h_s(\theta)]^2, \quad \theta\lesssim\theta_0 \tag{4}$$

and

$$\sigma(\theta)P(\theta)=2\,\mathrm{Im}h_s(\theta)\,\mathrm{Im}g_n(\theta), \quad \theta\lesssim\theta_0. \tag{5}$$

In this discussion it is important to recognize that the present measurements of $\sigma(\theta)$ and $\sigma(\theta)P(\theta)$ represent energy averages over an interval given by the energy spread of the incident neutron beam. Thus, for most of the elements in this study the averages will be over many resonances in the compound nucleus. In analyzing these data, instead of Eqs. (4) and (5) we must therefore use the relations

$$\langle\sigma(\theta)\rangle=\langle|g_n(\theta)|^2\rangle+[\mathrm{Im}h_s(\theta)]^2, \quad \theta\lesssim\theta_0 \tag{4'}$$

and

$$\langle\sigma(\theta)P(\theta)\rangle=2\,\mathrm{Im}h_s(\theta)\langle\mathrm{Im}g_n(\theta)\rangle, \quad \theta\lesssim\theta_0, \tag{5'}$$

where the angular parentheses denote the energy average. The electromagnetic amplitude $h_s(\theta)$ is virtually independent of energy over the averaging interval so that it is not necessary to distinguish between the average and the mean value for this quantity.

Values of $\langle\mathrm{Im}g_n(\theta)\rangle$ obtained from Eq. (5′) for the present measured values of $\langle\sigma(\theta)P(\theta)\rangle$ are found to be independent of θ for $\theta\lesssim 10°$ so that $\langle\mathrm{Im}g_n(\theta)\rangle$ can be replaced by $\langle\mathrm{Im}g_n(0°)\rangle$ in Eqs. (4′) and (5′). Furthermore, the numerical computations described in Sec. III A show that the assumptions leading to Eq. (3) are satisfied for $\theta_0\leqslant 10°$. Thus, it is consistent to take $\theta_0\approx 10°$ in Eqs. (4′) and (5′) with $\langle\mathrm{Im}g_n(\theta)\rangle$ replaced by $\langle\mathrm{Im}g_n(0°)\rangle$.

We now make use of the optical theorem

$$\mathrm{Im}g_n(0°)=k\sigma_t/4\pi, \tag{6}$$

where σ_t is the neutron total cross section, and write

TABLE III. Total neutron cross sections $\langle\sigma_t\rangle$, imaginary part of the forward nuclear scattering amplitude $\langle \mathrm{Im}g_n(0°)\rangle$, and upper limit on the real part of the forward nuclear-scattering amplitude $|\langle \mathrm{Re}g_n(0°)\rangle|$ at energies from 0.6–1.6 MeV for the nuclei in the present study. The errors shown are based on counting statistics only. Measured cross sections at all angles $\theta\lesssim 10°$ were utilized to determine the values of $|\langle \mathrm{Re}g_n(0°)\rangle|$.

Target nucleus	Energy (MeV)	$\langle\sigma_t\rangle$ (b)	$\langle \mathrm{Im}g_n(0°)\rangle$ (10^{-12} cm)	$\lvert\langle \mathrm{Re}g_n(0°)\rangle\rvert$ (10^{-12} cm)
U	0.6	7.88±0.14	1.06±0.02	0.84±0.02
	0.84	7.24±0.14	1.16±0.02	0.89±0.02
	1.0	6.96±0.10	1.21±0.02	0.78±0.02
	1.2	6.77±0.21	1.29±0.04	0.76±0.05
	1.6	6.92±0.15	1.53±0.03	0.72±0.05
Th	0.6	7.96±0.19	1.07±0.03	0.76±0.04
	0.84	6.95±0.18	1.11±0.03	0.79±0.03
	1.0	6.74±0.17	1.17±0.03	0.81±0.04
	1.2	6.43±0.22	1.23±0.04	0.78±0.05
	1.6	6.78±0.15	1.49±0.03	0.70±0.05
Pb	0.84	6.06±0.14	0.97±0.02	0.89±0.02
Au[a]	0.6	6.35±0.14	0.86±0.02	0.80±0.02
	0.84	6.07±0.13	0.97±0.02	0.73±0.03
	1.0	5.83±0.13	1.02±0.02	0.82±0.03
	1.2	5.82±0.12	1.11±0.02	0.75±0.03
	1.6	6.21±0.12	1.37±0.03	0.77±0.04
W	0.84	6.67±0.15	1.07±0.02	0.87±0.03
	1.0	7.01±0.18	1.22±0.03	0.50±0.06
	1.2	6.85±0.16	1.31±0.03	0.67±0.05
Cd	1.0	6.84±0.17	1.19±0.03	0.75±0.04

[a] Gold is not a spin-zero nucleus. Equation (2) in the text, from which the relations determining $|\langle \mathrm{Re}g_n(0)\rangle|$ follow, is only approximately valid.

Eq. (5′) in the form

$$\langle\sigma(\theta)P(\theta)\rangle = k\ \mathrm{Im}h_s(\theta)\langle\sigma_t\rangle/2\pi\,,\quad \theta\lesssim 10°. \tag{7}$$

This result is equivalent to the formula first obtained by Schwinger.[1] It shows the advantages of small-angle scattering as a polarization analyzer. This will be discussed further in Sec. III C.

Finally, we introduce the compound-elastic cross section $\sigma_{ce}(\theta)$, where

$$\sigma_{ce}(\theta)\equiv\langle|g_n(\theta)-\langle g_n(\theta)\rangle|^2\rangle\,, \tag{8}$$

and rewrite Eq. (4′) as

$$\langle\sigma(\theta)\rangle-[\mathrm{Im}h_s(\theta)]^2=\sigma_{ce}(\theta)+\langle \mathrm{Re}g_n(\theta)\rangle^2 + (k\langle\sigma_t\rangle/4\pi)^2\,,\quad \theta\lesssim 10°. \tag{9}$$

For the measurements reported here, the quantity $\langle\sigma(\theta)\rangle-[\mathrm{Im}h_s(\theta)]^2$ is virtually independent of θ for $\theta\lesssim 10°$ (as seen in Fig. 6). It follows from Eq. (9) that $\sigma_{ce}(\theta)+\langle \mathrm{Re}g_n(\theta)\rangle^2$ is independent of θ for $\theta\lesssim 10°$.

For measurements at energies such that many reaction channels are open, the unknown compound-elastic cross section is expected to be small compared with $|\langle g_n(0°)\rangle|^2$. This condition is approximately satisfied for most of the heavy nuclei that were used as targets in the present measurements. Thus, Eq. (9) with $\sigma_{ce}(\theta)$ set equal to zero, can be used to obtain a reasonable upper limit (i.e., one close to the true value) for the absolute value of the real part of the forward-scattering amplitude. Final values of $\langle \mathrm{Im}g_n(0°)\rangle$, calculated by use of Eq. (6), and upper limits for $|\langle \mathrm{Re}g_n(0°)\rangle|$, as given by Eq. (9), are listed in Table III. The errors shown in the table are based on counting statistics only. In the calculations of $|\langle \mathrm{Re}g_n(0°)\rangle|$, the quantities $(\langle\sigma(\theta)\rangle-[\mathrm{Im}h_n(\theta)]^2)$ for all $\theta\lesssim 10°$ were averaged to get the values shown in column 5.

C. Polarization in the ^{7}Li$(p,n)^7$Be Reaction

As pointed out in Sec. III B, Schwinger has shown that the polarization at small angles can be written in terms of the measured total and differential cross sections and the magnetic moment of the neutron. The more general approximation of Monahan and Elwyn[8] allows other interference terms to be taken into account as well. However, from the discussion in Sec. III A, the calculated values of polarization based on this formalism are not very sensitive to the actual values of the parameters of the nuclear interaction (at least for small values of the polarizability α) and are, in fact, insensitive to the parameters of the nuclear spin-orbit well. Thus, for an optical-model potential that gives a good representation of the total and differential cross section, the polarization calculated by the formula of Ref. 8 should give results almost identical to that calculated by Eq. (7). The values of polarization at small angles are therefore virtually model-independent; and consequently left/right asymmetry measurements in this angular region can serve as an analyzer[23] of the polarization of neutrons in the source reaction.

The necessity to modify the values of polarization $P_1(51°)$ in the ^{7}Li$(p,n)^7$Be reaction has been mentioned in Sec. III A. By use of Eq. (7) we have calculated the

TABLE IV. Values of $P_1(51°)$ for the ^{7}Li$(p,n)^7$Be reaction as a function of energy. Results are based on the use of each of the scattering samples as a polarization analyzer. The last column lists the weighted averages of the results in columns 3–8 at each energy. The errors shown are discussed in the text.

Proton energy (MeV)	Neutron energy (MeV)	$P_1(51°)$ U	Th	Pd	Au	W	Cd	$\langle P_1(51°)\rangle$
2.47	0.6	0.153±0.007	0.164±0.006	···	0.178±0.021	···	···	0.160±0.012
2.37	0.84	0.212±0.003	0.177±0.020	0.190±0.004	0.187±0.010	0.167±0.004	···	0.191±0.023
2.90	1.0	0.242±0.002	0.241±0.030	···	0.229±0.014	0.261±0.007	0.250±0.022	0.243±0.018
3.12	1.2	0.305±0.001	0.311±0.001	···	0.330±0.018	0.261±0.011	···	0.305±0.035
3.55	1.6	0.326±0.008	0.442±0.005	···	0.402±0.013	···	···	0.362±0.080

[23] R. G. P. Voss and R. Wilson, Phil. Mag. **1**, 175 (1956).

polarization expected in the scattering from each of the nuclei at all energies. From a least-squares fit of the measured polarization products $P_1(51°)P(\theta)$ to these expected polarizations, values of $P_1(51°)$ have been extracted. These values are shown in Table IV. The errors shown in columns 3–8 are standard deviations based on counting statistics. In Fig. 8, the weighted averages (column 9 of Table IV) of the values in columns 3–8 are compared with previously determined values[15,24] of $P_1(51°)$. Those values of $P_1(51°)$ utilized to determine the quantities $P(\theta)$ in Table II were taken from the smooth curve drawn through the points in Fig. 8. The results given in column 9 of Table IV (open circles) are smaller than most of the earlier measurements at energies below $E_p = 3.0$ MeV, although they do not disagree badly within the stated accuracy of the measurements. The uncertainties in the present average polarizations were determined from the extreme values observed in columns 3–8, and should be reliable estimates of the systematic errors that may exist in the measurements.

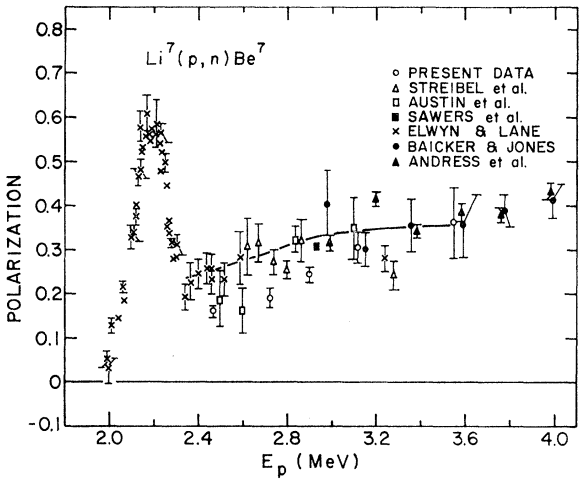

FIG. 8. Values of $P_1(51°)$ for the ^{7}Li$(p,n)^7$Be reaction. The present results (open circles) are from column 9 of Table IV. The previously measured values of $P_1(51°)$ are from Refs. 15 and 24.

IV. SUMMARY

The results of the present investigation, as discussed in Sec. III, may be summarized as follows:

(a) The measured angular and polarization distributions for the scattering of neutrons by Cd, W, Au, Pb, Th, and U at angles $\theta \lesssim 15°$ are consistent with calculations based on a neutron-nucleus interaction that is represented by a potential containing contributions from the known long-range electromagnetic interactions as well as from the short-range specifically nuclear force. There is therefore no evidence for the existence of any anomalous small-angle behavior of the cross section at energies between 0.6 and 1.6 MeV.

(b) Measured differential cross sections in the small-angle scattering region can be utilized, along with total cross-section measurements, to determine both the imaginary part and an upper limit for the absolute value of the real part of the forward nuclear scattering amplitude.

(c) The measured left/right asymmetries in the scattering process at small angles have been utilized to obtain quite accurate values of the polarization $P_1(51°)$ in the ^{7}Li$(p,n)^7$Be source reaction. For the samples used in these measurements, the polarization in scattering at small angles is very large, reasonably energy-independent, and virtually independent of the details of the model chosen to represent the nuclear interaction. Hence measurements in this range can be more accurate than the conventional large-angle scattering techniques for determining the source polarization in various neutron-production reactions. Indeed, in an experimental setup in which the scattering at a number of angles can be determined simultaneously, the advantages of small-angle investigations may outweigh the experimental difficulties associated with such measurements.

In connection with result (b) above, further studies are in progress to investigate whether a knowledge of the forward-scattering amplitudes can be used to determine compound-elastic scattering cross sections in the small-angle region. The utility of measured forward-scattering amplitudes for the determination of a possible long-range contribution to the nuclear optical potential[25] is also under investigation.

ACKNOWLEDGMENTS

We wish to thank R. Amrein and the crew of the Van de Graaff generator for operation of the accelerator and W. J. Ray and V. Blair for their assistance with the experiment.

[24] H. R. Striebel, S. E. Darden, and W. Haeberli, Nucl. Phys. **6**, 188 (1958); J. A. Baicker and K. W. Jones, *ibid.* **17**, 424 (1960); W. D. Andress, F. O. Purser, J. R. Sawers, and R. L. Walter, *ibid.* **70**, 313 (1965); J. R. Sawers, G. L. Morgan, L. A. Schaller, and R. L. Walter, Phys. Rev. **168**, 1102 (1968).

[25] R. Fox, Nucl. Phys. **43**, 110 (1963).